

Opposing roles for p16^{Ink4a} and p19^{Arf} in senescence and ageing caused by BubR1 insufficiency

Darren J. Baker¹, Carmen Perez-Terzic², Fang Jin¹, Kevin Pitel¹, Nicolas J. Niederländer³, Karthik Jeganathan¹, Satsuki Yamada³, Santiago Reyes³, Lois Rowe³, H. Jay Hiddinga⁴, Norman L. Eberhardt⁴, Andre Terzic³ and Jan M. van Deursen^{1,4,5}

Expression of p16^{Ink4a} and p19^{Arf} increases with age in both rodent and human tissues. However, whether these tumour suppressors are effectors of ageing remains unclear, mainly because knockout mice lacking p16^{Ink4a} or p19^{Arf} die early of tumours. Here, we show that skeletal muscle and fat, two tissues that develop early ageing-associated phenotypes in response to BubR1 insufficiency, have high levels of p16^{Ink4a} and p19^{Arf}. Inactivation of p16^{Ink4a} in BubR1-insufficient mice attenuates both cellular senescence and premature ageing in these tissues. Conversely, p19^{Arf} inactivation exacerbates senescence and ageing in BubR1 mutant mice. Thus, we identify BubR1 insufficiency as a trigger for activation of the *Cdkn2a* locus in certain mouse tissues, and demonstrate that p16^{Ink4a} is an effector and p19^{Arf} an attenuator of senescence and ageing in these tissues.

Cellular senescence is a state of irreversible growth arrest that can be induced by various cellular stressors^{1,2}. The *Cdkn2a* locus encodes two separate tumour suppressors, p16^{Ink4a} (A001711), a cyclin-dependent kinase (Cdk) inhibitor that can block G₁-S progression when present above a certain level, and p19^{Arf} (A001713), a positive regulator of the transcription factor p53 that integrates and responds to a wide variety of cellular stresses^{1,3-5}. Both p16^{Ink4a} and p19^{Arf} are effectors of senescence in cultured cells⁶ and their levels increase with ageing in many tissues^{7,8}. This has led to speculation that their induction is causally implicated in *in vivo* senescence and organismal ageing. However, rigorous testing of this notion has been difficult because mice that lack p16^{Ink4a} or p19^{Arf} die of cancer long before they reach the age at which normal mice start to develop age-related disorders^{1,2}. Recent evidence in middle-aged p16^{Ink4a} knockout mice indicates that the age-induced expression of p16^{Ink4a} limits the proliferative and regenerative capacity of progenitor populations⁹⁻¹¹. Yet, whether the increased stem-cell proliferation and tissue regeneration seen in p16^{Ink4a} knockouts actually delay onset of age-related pathologies remains unknown because of the limited animal lifespan^{1,12}.

One approach to study the role of p16^{Ink4a} and p19^{Arf} in ageing would be to determine whether their respective inactivation by single gene mutations, in mouse models that develop ageing-associated pathologies at an early age, would prevent or delay premature ageing. Mutant mice with low levels of the mitotic checkpoint protein BubR1 (called BubR1 hypomorphic or *BubR1*^{HH} mice, A003172) undergo premature separation of sister chromosomes and develop progressive aneuploidy along

with various progeroid phenotypes that include short lifespan, cachectic dwarfism, lordokyphosis (abnormal curvature of the spine), sarcopaenia (age-related skeletal muscle atrophy), cataracts, craniofacial dysmorphisms, arterial stiffening, loss of (subcutaneous) fat, reduced stress tolerance and impaired wound healing¹³⁻¹⁵. During the course of natural ageing, several mouse tissues show a marked decline in BubR1 protein expression, which, combined with the observation that *BubR1*^{HH} mice age prematurely, suggests a possible role for BubR1 in regulating natural ageing¹³⁻¹⁵. Here we show that certain mouse tissues induce p16^{Ink4a} and p19^{Arf} in response to BubR1 hypomorphism. Using *BubR1*^{HH} mice in which these tumour suppressors are lacking, we have demonstrated that p16^{Ink4a} is an effector of cellular senescence and ageing, whereas, p19^{Arf} acts to suppress cellular senescence and ageing.

RESULTS

p16^{Ink4a} inactivation increases the lifespan of *BubR1*^{HH} mice

To determine the requirement for p16^{Ink4a} in the development of progeroid phenotypes in BubR1-insufficient mice, we bred *BubR1*^{HH} mice on a p16^{Ink4a} homozygous-null genetic background. In total, 86 *BubR1*^{HH}, p16^{Ink4a}^{-/-}, 192 *BubR1*^{HH}, 160 *BubR1*^{+/+} and 44 p16^{Ink4a}^{-/-} mice were generated and monitored for development of age-related phenotypes for a period of one year. Inactivation of p16^{Ink4a} extended the lifespan of *BubR1*^{HH} mice by 25% (Fig. 1a). Although the median lifespan of *BubR1*^{HH} mice was extended in the absence of p16^{Ink4a}, the maximum lifespan was not, suggesting that the condition(s) that cause(s) death was not rescued by p16^{Ink4a} inactivation.

¹Department of Pediatric and Adolescent Medicine, ²Department of Physical Medicine and Rehabilitation, ³Department of Medicine and ⁴Department of Biochemistry and Molecular Biology Mayo Clinic College of Medicine, Rochester, MN 55905, USA.

⁵Correspondence should be addressed to J.M.v.D. (e-mail: vandeursen.jan@mayo.edu)

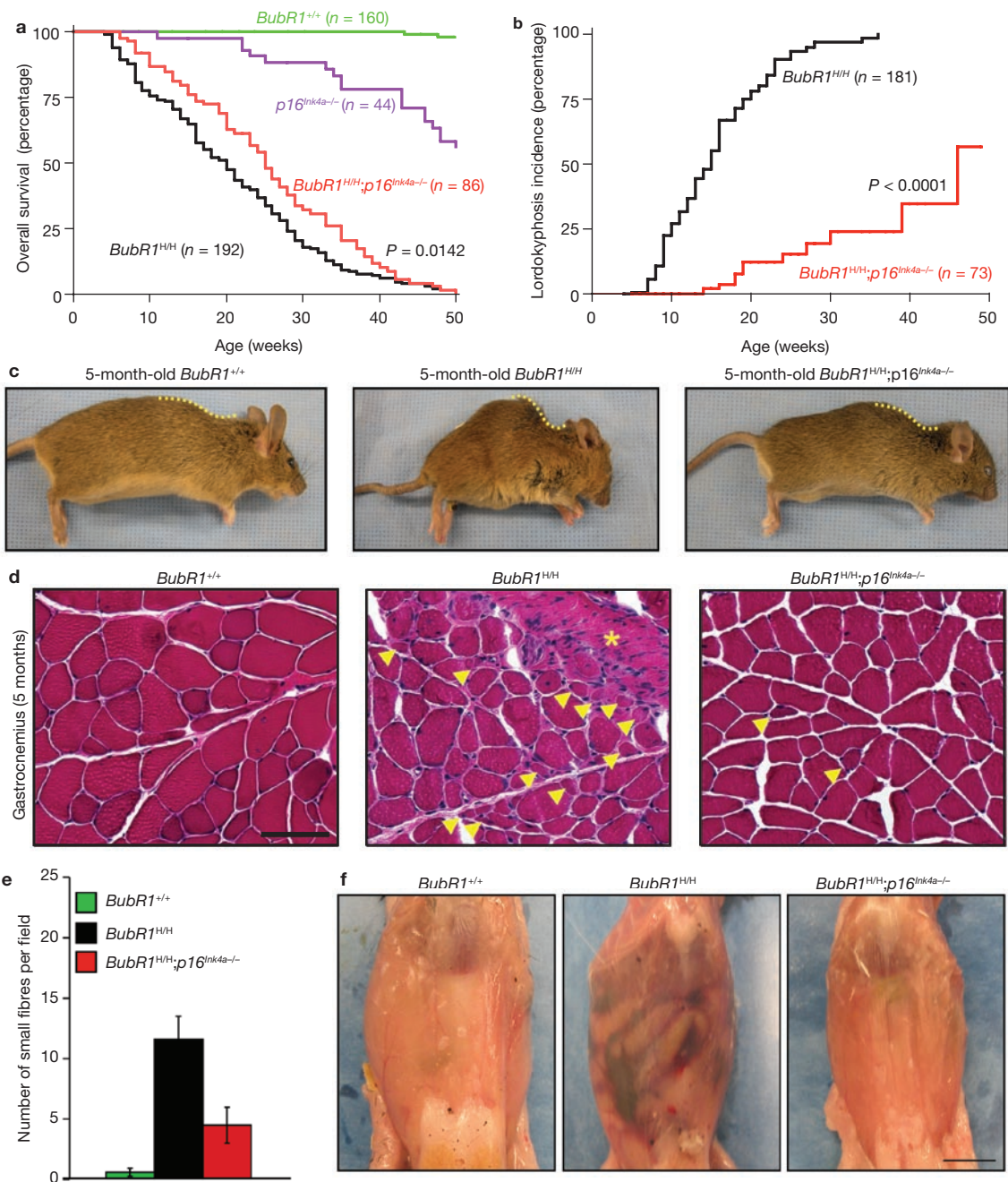


Figure 1 Ablation of $p16^{Ink4a}$ in $BubR1^{H/H}$ mice extends lifespan and attenuates sarcopaenia. **(a)** Overall survival curves for wild-type, $p16^{Ink4a-/-}$, $BubR1^{H/H}$ and $BubR1^{H/H};p16^{Ink4a-/-}$ mice. The median overall survival of combined $BubR1^{H/H};p16^{Ink4a-/-}$ mice is 25 weeks, a 25% extension in lifespan compared with $BubR1^{H/H}$ animals. We note that the $p16^{Ink4a-/-}$, $BubR1^{H/H}$ and $BubR1^{H/H};p16^{Ink4a-/-}$ curves are all significantly different from the wild-type ($BubR1^{+/+}$) curve ($P < 0.0001$, log-rank tests). Moreover, the $BubR1^{H/H};p16^{Ink4a-/-}$ curve is significantly different from the $BubR1^{H/H}$ curve ($P = 0.0142$). **(b)** Incidence and latency of lordokyphosis in $BubR1^{H/H}$ and $BubR1^{H/H};p16^{Ink4a-/-}$ mice. The curves are significantly different ($P < 0.0001$, log-rank test). We note that no wild-type or $p16^{Ink4a-/-}$ mice developed lordokyphosis during our one-year observation period (data not shown).

$p16^{Ink4a}$ loss blunts sarcopaenia induced by BubR1 insufficiency

A prominent ageing-associated phenotype of $BubR1^{H/H}$ mice is the development of lordokyphosis¹³. The incidence of this phenotype was

markedly reduced in $BubR1^{H/H};p16^{Ink4a-/-}$ animals when compared with $BubR1^{H/H}$ mice (Fig. 1b, c). Furthermore, the median time to onset of lordokyphosis was three times longer in $BubR1^{H/H};p16^{Ink4a-/-}$ mice

markedly reduced in $BubR1^{H/H};p16^{Ink4a-/-}$ animals when compared with $BubR1^{H/H}$ mice (Fig. 1b, c). Furthermore, the median time to onset of lordokyphosis was three times longer in $BubR1^{H/H};p16^{Ink4a-/-}$ mice

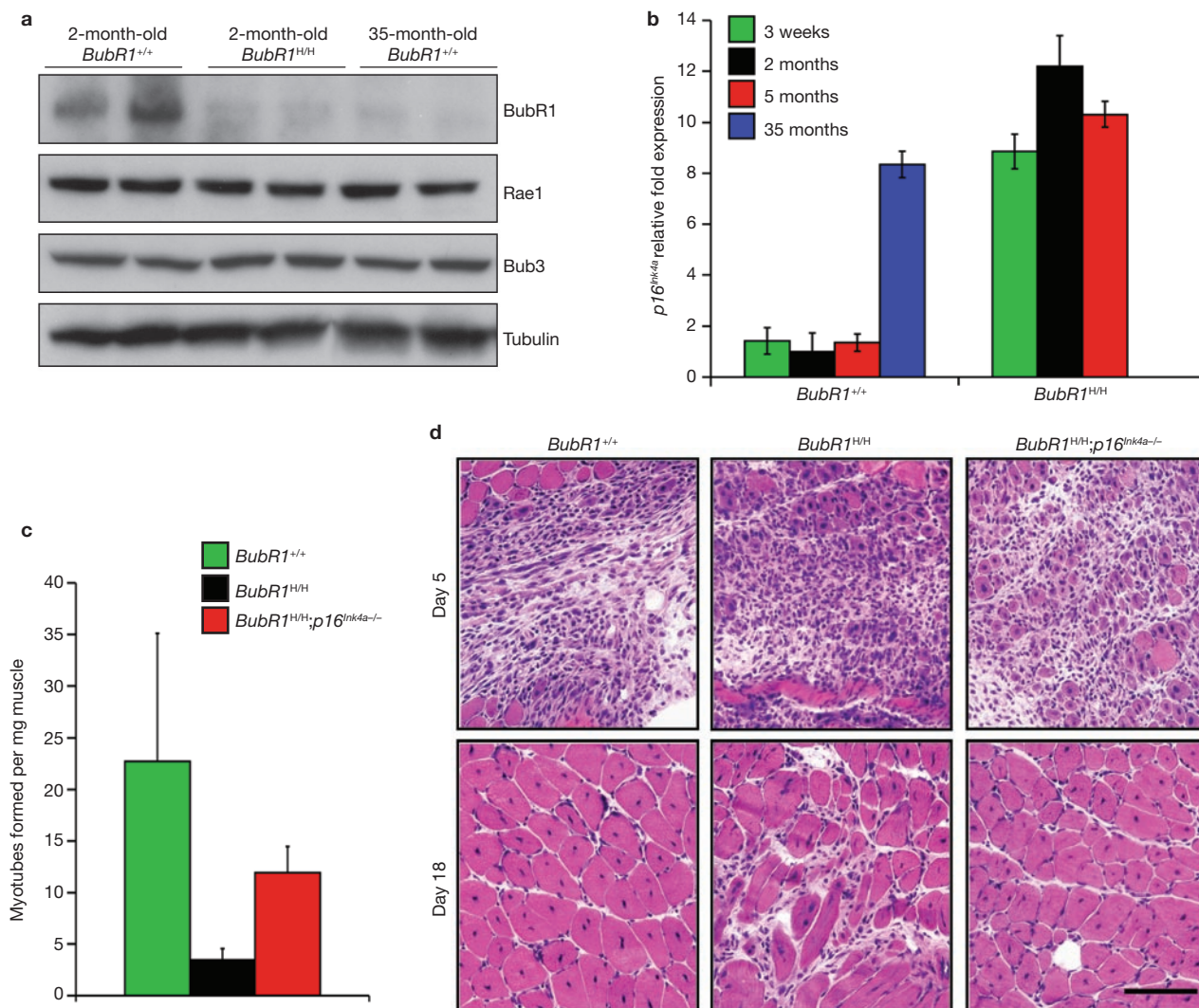


Figure 2 Inverse correlation between BubR1 and p16^{Ink4a} expression levels with ageing. **(a)** Western blot analysis of gastrocnemius muscle in young wild-type and *BubR1*^{H/H} mice and old wild-type mice. Blots were probed with antibodies against BubR1, Bub3 and Rae1. Anti-tubulin was used as a loading control. Note that the mitotic checkpoint proteins Bub3 and Rae1 remain highly expressed as wild-type mice age. Uncropped images of the scans are shown in Supplementary Information, Fig. S6a. **(b)** p16^{Ink4a} expression in wild-type and *BubR1*^{H/H} gastrocnemius muscles at various ages analysed by qRT-PCR. Data are mean \pm s.d. ($n = 3$ males per genotype and age group, with triplicate measurements taken). Values were normalized to *GAPDH*. Relative

fold expression is to 2-month-old wild-type values. **(c)** Myotube formation potential of gastrocnemius muscles from 5-month-old mice of the indicated genotypes analysed by a well-standardized *in vitro* assay. Data are mean \pm s.d. ($n = 4$). **(d)** Cardiotoxin-treated gastrocnemius muscle of 5-month-old wild-type, *BubR1*^{H/H} and *BubR1*^{H/H};p16^{Ink4a}^{-/-} mice at 5 or 18 days after injection. Note that all gastrocnemius muscles show an extensive hypercellular response to cardiotoxin injection by day 5 regardless of genotype. Wild-type and *BubR1*^{H/H};p16^{Ink4a}^{-/-} mice have complete restoration of muscle architecture by myofibres with central nuclei by day 18, whereas *BubR1*^{H/H} mice have been unable to restore normal tissue structure. Scale bar is 100 μ m.

than in *BubR1*^{H/H} mice (Fig. 1b). Lordokyphosis is associated with both osteoporosis and age-related degenerative loss of muscle mass and strength (sarcopaenia) in wild-type mice of extremely advanced age¹⁶. Histological evaluation of longitudinal femur sections from kyphotic *BubR1*^{H/H} mice revealed no evidence for osteoporosis (Supplementary Information, Fig. S1a, b). Histopathology on gastrocnemius and paraspinal muscles of 5-month-old *BubR1*^{H/H} mice, however, revealed clear signs of skeletal muscle atrophy and degeneration (Fig. 1d and data not shown). Muscle degeneration was greatly reduced in *BubR1*^{H/H} muscles lacking p16^{Ink4a} (Fig. 1d, e). In addition, abdominal muscles of *BubR1*^{H/H} mice were poorly developed, as revealed by macroscopic analysis and magnetic resonance imaging (Fig. 1f; Supplementary Information, Fig. S1c). Depletion of p16^{Ink4a} resulted in substantial

correction of this defect. These data demonstrate that p16^{Ink4a} has a major role in establishing sarcopaenia in *BubR1*^{H/H} mice.

p16^{Ink4a} limits the regenerative capacity of β cells and has been linked to pancreatic islet atrophy and development of diabetes^{9,17,18}, which in turn can cause muscle atrophy through accelerated degradation of muscle protein¹⁹. This prompted us to test whether the sarcopaenia observed in *BubR1*^{H/H} mice might be due to β cell failure. *BubR1*^{H/H} mice showed highly efficient glucose clearance in a glucose-tolerance test (Supplementary Information, Fig. S2a). Complementary blood insulin measurements indicated that insulin sensitivity was not impaired in *BubR1*^{H/H} mice and showed no evidence for insulin resistance (Supplementary Information, Fig. S2b). Furthermore, overall pancreatic morphology, as well as islet size, shape and abundance were similar

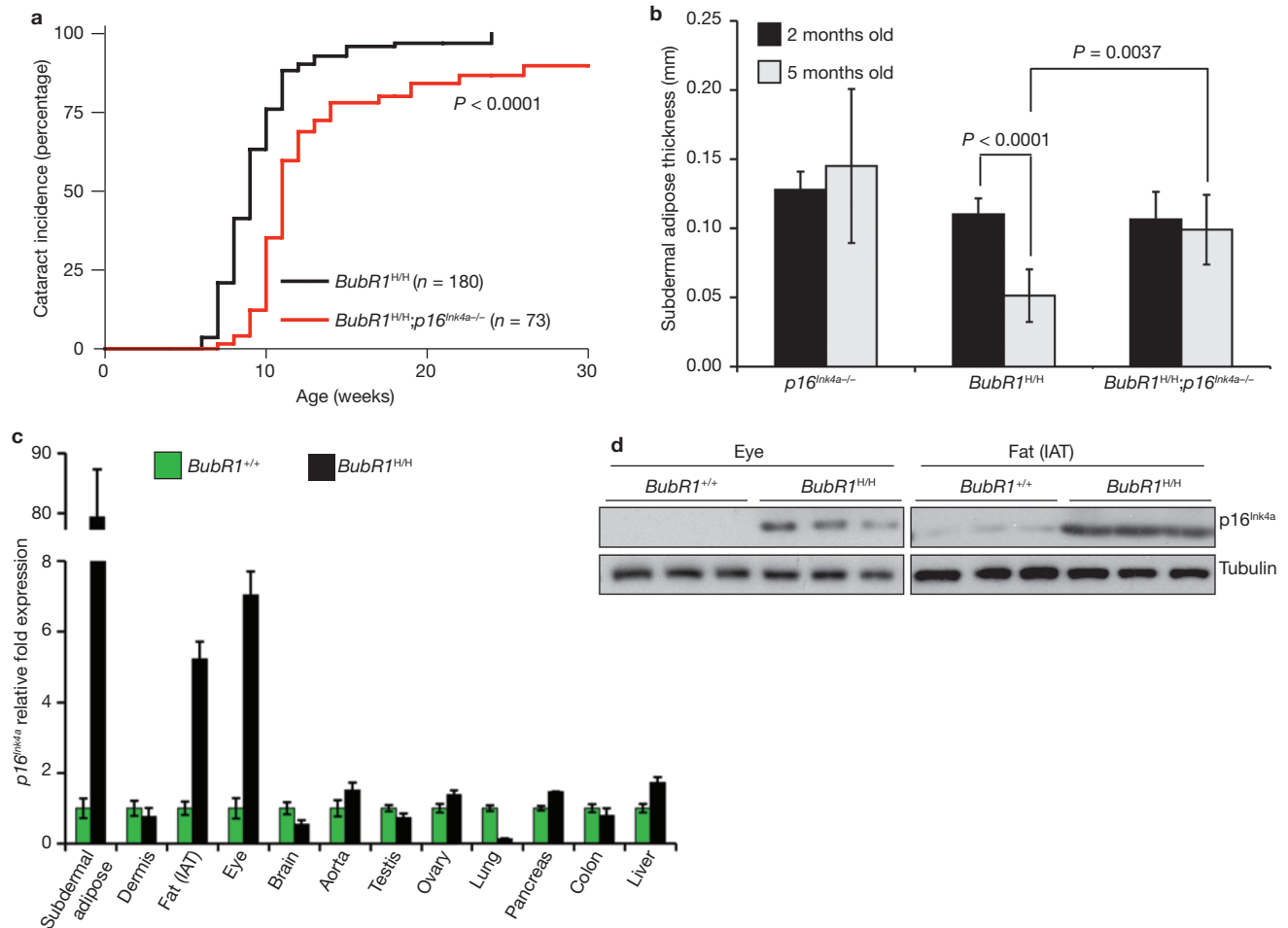


Figure 3 *p16^{Ink4a}* disruption attenuates selective progeroid features of *BubR1* hypomorphic mice. **(a)** Incidence and latency of cataract formation in *BubR1^{H/H}* and *BubR1^{H/H};p16^{Ink4a}^{-/-}* mice as detected by the use of slit light after dilation of eyes. The curves are significantly different ($P < 0.0001$, log-rank test). We note that no wild-type or *p16^{Ink4a}^{-/-}* mice developed cataracts during this observation period. **(b)** Subcutaneous adipose layer thickness of *p16^{Ink4a}^{-/-}*, *BubR1^{H/H}* and *BubR1^{H/H};p16^{Ink4a}^{-/-}* mice at 2 and 5 months of age. Data are mean \pm s.d. ($n = 4$ male mice for each age per genotype). A two-tailed Mann-Whitney test

was used for statistical analysis. **(c)** qRT-PCR analysis for relative expression of *p16^{Ink4a}* in a variety of 2-month-old tissues from *BubR1^{H/H}* and wild-type mice. Values were normalized to *GAPDH*, and relative fold is to 2-month-old wild-type samples. Data are mean \pm s.d. ($n = 3$ male mice for each tissue, with triplicate measurements taken). **(d)** Western blots of eye and fat extracts from 2-month-old *BubR1^{+/+}* and *BubR1^{H/H}* mice probed with anti-*p16^{Ink4a}* antibody. Anti-tubulin antibody served as loading control. Uncropped images of the scans are shown in Supplementary Information, Fig. S6b, c.

in 12-month-old *BubR1^{H/H}* and control mice, as verified by histology (Supplementary Information, Fig. S2c). Consistently, *p16^{Ink4a}* expression in the pancreas was not significantly elevated in *BubR1^{H/H}* mice, compared with *BubR1^{+/+}* counterparts. Thus, sarcopaenia in *BubR1^{H/H}* mice is unlikely to be caused by *p16^{Ink4a}*-mediated β cell degeneration or insulin resistance.

BubR1 and *p16^{Ink4a}* levels are inversely linked in skeletal muscle

To determine whether *BubR1* may have a role in normal skeletal muscle ageing, we measured *BubR1* protein levels in skeletal muscle of young and old wild-type mice by western blot analysis. Gastrocnemius muscles had considerably higher levels of *BubR1* protein at 2 months than at 35 months of age (Fig. 2a; Supplementary Information, Fig. S6a). *BubR1* transcripts were undetectable by qRT-PCR in the gastrocnemius of 35-month-old mice but were readily present at 2 months (data not shown), suggesting that reduced *BubR1* transcriptional activity contributes to the decline in *BubR1* protein levels at advanced age. In contrast to *BubR1* transcription, *p16^{Ink4a}* transcription increased markedly with age

in gastrocnemius muscles of old wild-type mice (Fig. 2b). Gastrocnemius of 2- and 5-month-old *BubR1^{H/H}* mice also had high *p16^{Ink4a}* transcript levels (Fig. 2b), providing evidence for an inverse relationship between *BubR1* and *p16^{Ink4a}* expression. To characterize this relationship further, we measured *p16^{Ink4a}* expression in gastrocnemius of 3-week-old *BubR1^{H/H}* mice, when skeletal muscle atrophy is histologically undetectable (Supplementary Information, Fig. S2d). Transcript levels of *p16^{Ink4a}* were similarly elevated for 3-week-old, and 2- and 5-month-old mice (Fig. 2b), indicating that *p16^{Ink4a}* induction is an early response to *BubR1* hypomorphism that precedes histological signs of sarcopaenia.

Increased expression of *p16^{Ink4a}* with age in adult stem cells is associated with reduced tissue repair and regeneration in several mouse tissues^{9–12}. To explore whether *p16^{Ink4a}*-mediated exhaustion of myogenic stem-cell potential might contribute to premature sarcopaenia in *BubR1^{H/H}* mice, *in vitro* myoblast-to-myofibre differentiation assays were performed on gastrocnemius muscles from 5-month-old wild-type, *BubR1^{H/H}* and *BubR1^{H/H};p16^{Ink4a}^{-/-}* mice. In these assays, the average number of myotubes obtained per milligram of muscle tissue was about 7-fold lower in

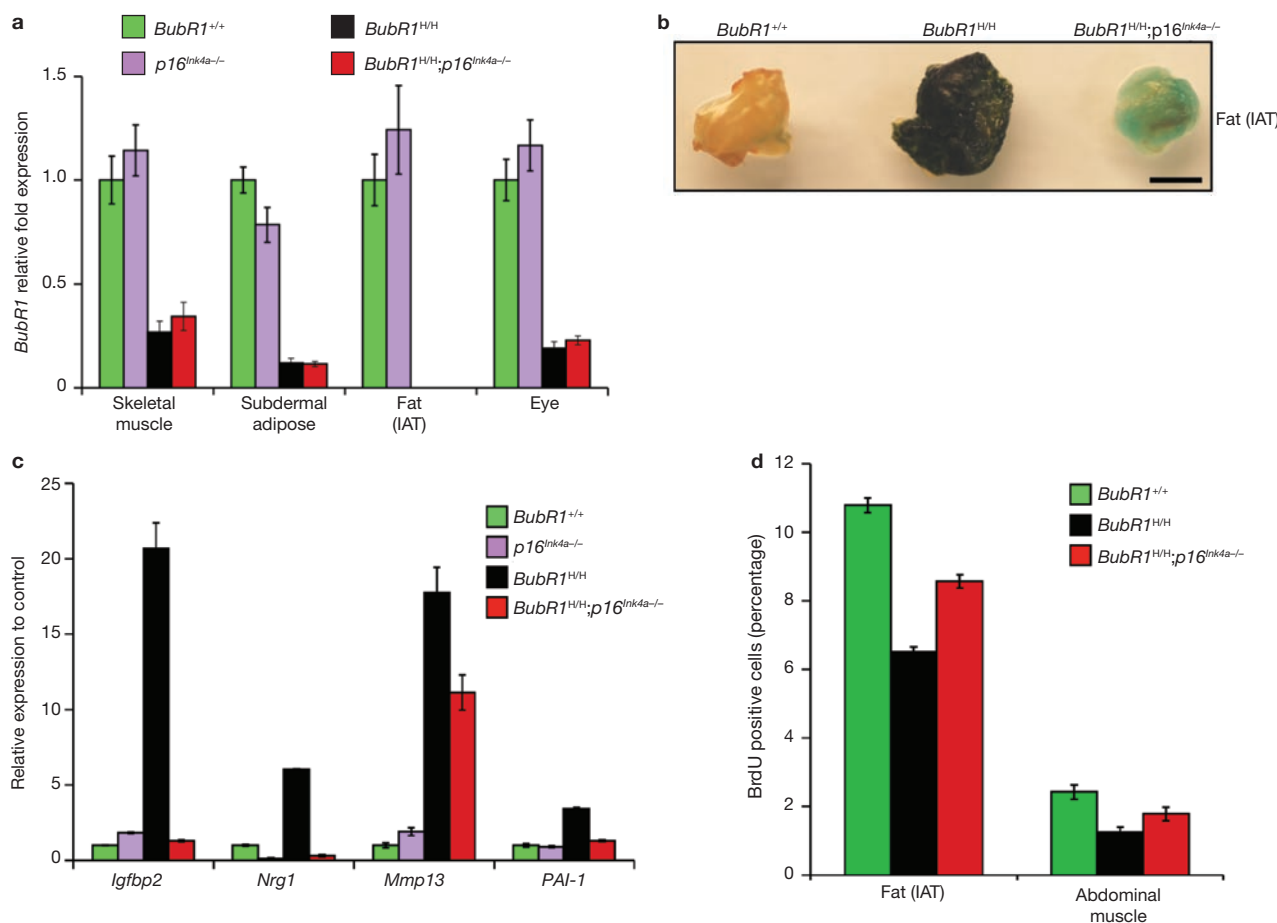


Figure 4 *p16*^{Ink4a} induction in *BubR1*^{H/H} mice promotes cellular senescence.

(a) Relative expression of BubR1 in gastrocnemius, subdermal adipose, fat deposits and eyes from 2-month-old wild-type, *p16*^{Ink4a-/-}, *BubR1*^{H/H} and *BubR1*^{H/H};*p16*^{Ink4a-/-} mice as determined by qRT-PCR. Values were normalized to GAPDH. Relative fold is to 2-month-old wild-type samples. Data are mean \pm s.d. ($n = 3$ male mice per genotype, with triplicate measurements taken per sample). We note that ablation of *p16*^{Ink4a} was unable to increase the amount of BubR1 present in either wild-type or *BubR1* hypomorphic mice. (b) IAT of 5-month-old wild-type, *BubR1*^{H/H}

and *BubR1*^{H/H};*p16*^{Ink4a-/-} mice stained for SA- β -galactosidase activity. Scale bar is 2 mm. (c) Relative expression of senescence markers in gastrocnemius muscles of 2-month-old wild-type, *p16*^{Ink4a-/-}, *BubR1*^{H/H} and *BubR1*^{H/H};*p16*^{Ink4a-/-} mice analysed by qRT-PCR. Data are mean \pm s.d. ($n = 3$ male mice per genotype). Values were normalized to GAPDH. Relative fold expression is to 2-month-old wild-type muscle. (d) Analysis of replicative senescence in skeletal muscle and fat of 2-month-old wild-type, *BubR1*^{H/H} and *BubR1*^{H/H};*p16*^{Ink4a-/-} mice by analysing *in vivo* BrdU incorporation. Data are mean \pm s.d. ($n = 3$ males per genotype).

BubR1^{H/H} mice than in wild-type mice (Fig. 2c). By contrast, only a 2-fold reduction in myotube formation was observed in *BubR1*^{H/H} mice lacking *p16*^{Ink4a}. To confirm these data, 5-month-old wild-type, *BubR1*^{H/H} and *BubR1*^{H/H};*p16*^{Ink4a-/-} mice were challenged to regenerate muscle fibres by injection of cardiotoxin, a 60-amino-acid polypeptide that causes acute injury by rapidly destroying muscle fibres²⁰. Consistent with our *in vitro* data, muscle regeneration was overtly delayed in *BubR1*^{H/H} mice, but not in *BubR1*^{H/H};*p16*^{Ink4a-/-} counterparts (Fig. 2d). Collectively, these data indicate that *p16*^{Ink4a} promotes sarcopaenia in *BubR1*^{H/H} mice, at least in part, by impairing muscle regeneration.

p16^{Ink4a} loss attenuates ageing in selective *BubR1* hypomorphic tissues

Loss of *p16*^{Ink4a} caused a modest, yet significant, delay in the latency of cataract formation in *BubR1*^{H/H} mice (Fig. 3a). Aged skin is characterized by reduced dermal thickness and subcutaneous adipose tissue, both of which are observed in *BubR1*^{H/H} mice at young ages¹³. At 2 months of age, *BubR1*^{H/H}, *BubR1*^{H/H};*p16*^{Ink4a-/-} and *p16*^{Ink4a-/-} mice had similar amounts

of subdermal adipose tissue (Fig. 3b). As expected, the mean thickness of the subcutaneous adipose layer decreased notably in 5-month-old *BubR1*^{H/H} mice. This decline was not accompanied by increased fat storage in liver tissue (Supplementary Information, Fig. S2e). The decrease in subcutaneous fat was much less severe in age-matched *BubR1*^{H/H};*p16*^{Ink4a-/-} mice (Fig. 3b), indicating that *p16*^{Ink4a} is, at least in part, responsible for loss of subcutaneous adipose tissue in *BubR1*^{H/H} mice. Tolerance of anaesthetic stress was also greatly improved in *BubR1*^{H/H};*p16*^{Ink4a-/-} mice (Supplementary Information, Table S1), as was adipose tissue deposition (Supplementary Information, Fig. S2f). However, several progeroid symptoms seen in *BubR1*^{H/H} mice remained unchanged following loss of *p16*^{Ink4a}, including dwarfism, dermal thinning, arterial wall stiffening and infertility (Supplementary Information, Table S1 and data not shown). No progeroid phenotypes of *BubR1*^{H/H} mice were aggravated by *p16*^{Ink4a} loss.

The differential corrective effects of *p16*^{Ink4a} disruption on individual progeroid phenotypes suggest tissue-specific differences in engagement of the *p16*^{Ink4a} pathway in the cellular response to BubR1 deficiency. *BubR1*^{H/H} tissues in which *p16*^{Ink4a} loss causes a significant

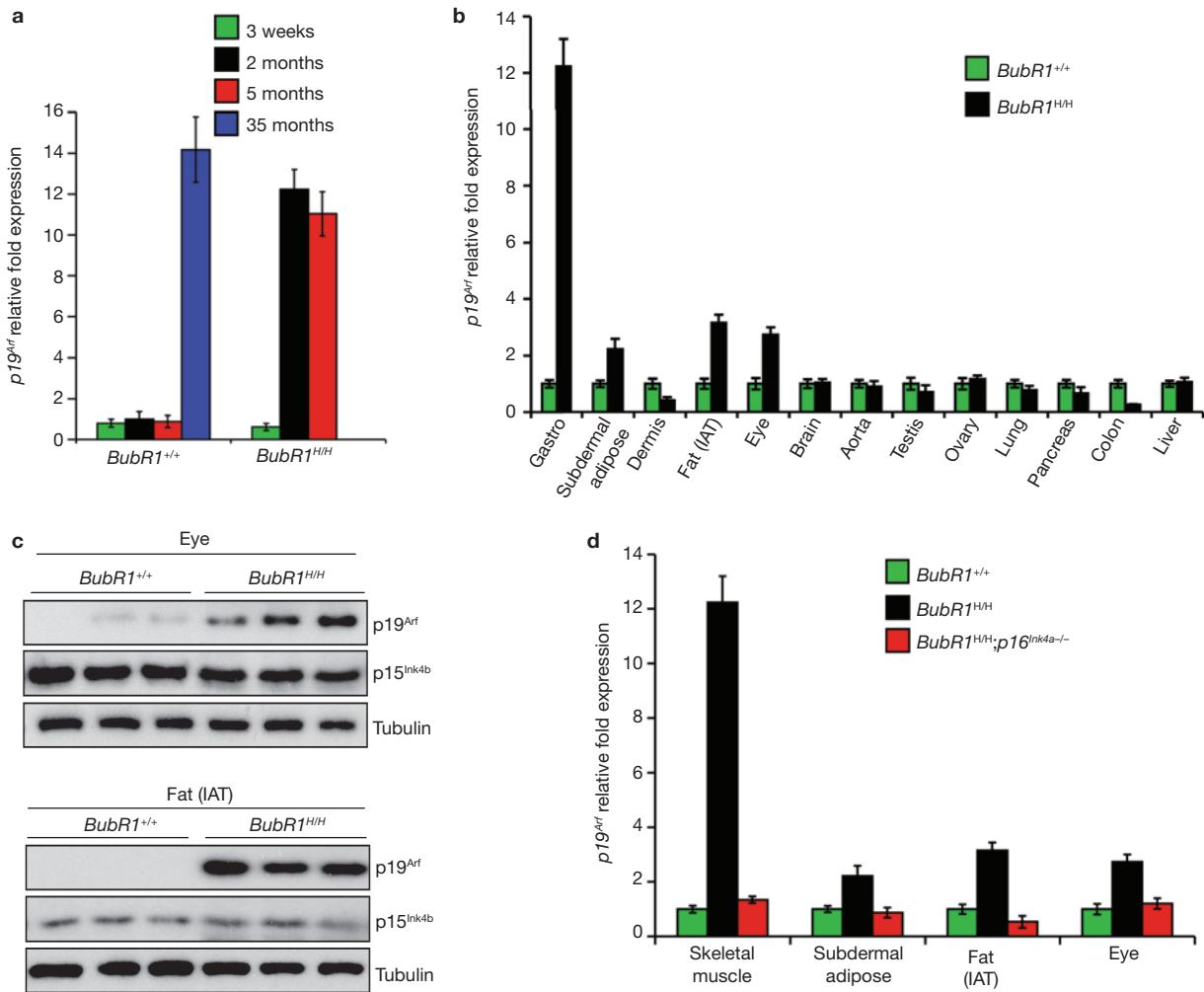


Figure 5 $p19^{Arf}$ is elevated in *BubR1* hypomorphic tissues with high $p16^{Ink4a}$. (a) Skeletal muscles of wild-type and *BubR1^{HHH}* mice of various ages were analysed for $p19^{Arf}$ expression by qRT-PCR. All values were normalized to *GAPDH*. Data are mean \pm s.d. ($n = 3$ mice were used per genotype and age group). (b) Relative expression of $p19^{Arf}$ in various tissues of 2-month-old *BubR1^{HHH}* and *BubR1^{+/+}* mice as measured by qRT-PCR. Data are mean \pm s.d. ($n = 3$ males per genotype). All values were normalized to *GAPDH*. Relative expression is to wild-type samples. (c) Western blots of

eye and fat extracts from 2-month-old *BubR1^{+/+}* and *BubR1^{HHH}* mice probed with anti- $p19^{Arf}$ and $p15^{Ink4b}$ antibodies. Anti-tubulin antibody was used as a loading control. Uncropped images of the scans are shown in Supplementary Information, Fig. S6b, c. (d) Relative expression of $p19^{Arf}$ in skeletal muscle (gastrocnemius), subdermal adipose, fat deposits and eyes of 2-month-old wild-type, *BubR1^{HHH}* and *BubR1^{HHH};p16^{Ink4a}^{-/-}* mice as determined by qRT-PCR. Data are mean \pm s.d. ($n = 3$ males per genotype). All values were normalized to *GAPDH*. Relative expression is to wild-type samples.

delay of premature ageing, such as eye and (subdermal) adipose tissue, showed strong induction of $p16^{Ink4a}$ expression in response to *BubR1* hypomorphism (Fig. 3c, d; Supplementary Information, Fig. S6b, c). *BubR1^{HHH}* tissues in which $p16^{Ink4a}$ inactivation has no discernible corrective effect, such as dermis, brain, aorta, testis and ovary, did not exhibit significant $p16^{Ink4a}$ induction (Fig. 3c and data not shown). Furthermore, mutant tissues that are not subjected to premature ageing, including lung, pancreas, colon and liver¹³, maintained low $p16^{Ink4a}$ expression levels. Together, these data demonstrate that $p16^{Ink4a}$ is activated in a subset of tissues in *BubR1^{HHH}* mice, where it contributes to progeroid phenotypes.

$p16^{Ink4a}$ loss attenuates *in vivo* senescence

BubR1 is a putative E2F-regulated gene²¹ and loss of $p16^{Ink4a}$ leads to increased E2F transcriptional activity²². Accordingly, attenuation of ageing in skeletal muscle, fat and eye may be the result of increased *BubR1*

gene expression. However, this is unlikely as *BubR1* transcript levels in these tissues were not affected by loss of $p16^{Ink4a}$ (Fig. 4a). As $p16^{Ink4a}$ is an effector of cellular senescence, $p16^{Ink4a}$ deletion may delay ageing in hypomorphic mice by decreasing senescence. As shown in Fig. 4b, *BubR1^{HHH}* adipose tissue expresses high levels of senescence-associated (SA)- β -galactosidase, a marker of cellular senescence²³. SA- β -galactosidase staining was much lower in adipose tissue of *BubR1^{HHH};p16^{Ink4a}^{-/-}* mice (Fig. 4b). Skeletal muscles of 2-month-old *BubR1^{HHH}* mice did not stain positive for SA- β -galactosidase but expressed high levels of several other senescence-associated genes, including *Igf1bp2*, *Nrg1*, *Mmp13* and *PAI-1²⁴⁻²⁷* (Fig. 4c). Expression of these markers was decreased markedly in skeletal muscles of age-matched *BubR1^{HHH};p16^{Ink4a}^{-/-}* mice. A key feature of senescence is loss of proliferative potential. *In vivo* 5-bromo-2-deoxyuridine (BrdU) labelling showed that 2-month-old *BubR1^{HHH}* mice had much lower percentages of cycling cells in skeletal muscle and fat than wild-type mice (Fig. 4d). These reductions were less profound in

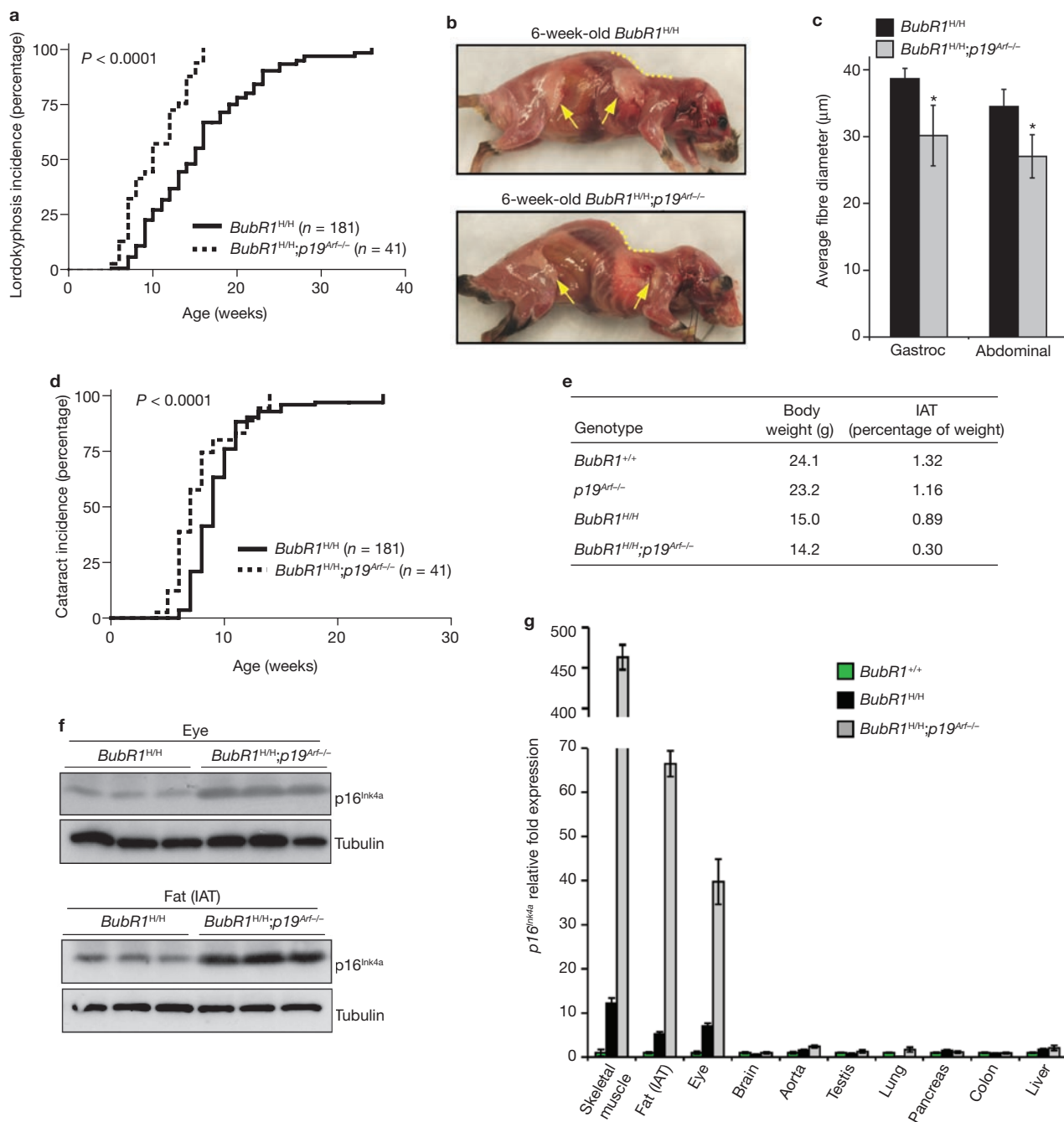


Figure 6 Accelerated ageing in *BubR1*^{H/H} mouse tissues with increased *p16*^{Ink4a} expression when *p19*^{Arf} is lacking. **(a)** Incidence and latency of lordokypnosis in *BubR1*^{H/H} and *BubR1*^{H/H};*p19*^{Arf/-} mice. The curves are significantly different ($P < 0.0001$, log-rank test). **(b)** Skinned 6-week-old *BubR1*^{H/H} and *BubR1*^{H/H};*p19*^{Arf/-} males. Note that the *BubR1*^{H/H};*p19*^{Arf/-} mouse has more profound lordokypnosis (dotted line) and reduced subcutaneous fat deposits (arrows). **(c)** Average muscle fibre size of gastrocnemius (Gastroc) and abdominal muscles of *BubR1*^{H/H} and *BubR1*^{H/H};*p19*^{Arf/-} males. Data are mean \pm s.d. ($n = 3$ mice per genotype). A two-tailed Mann-Whitney test was used for statistics. For both comparisons, $P < 0.0001$. **(d)** Incidence and latency of cataract formation in *BubR1*^{H/H}

and *BubR1*^{H/H};*p19*^{Arf/-} mice. The curves are significantly different ($P < 0.0001$, log-rank test). **(e)** Amount of inguinal adipose tissue in 6-week-old mice of the indicated genotypes. IAT is expressed as percentage of total body weight. Three male mice of each genotype were used. **(f)** Western blots of eye and fat extracts from 2-month-old *BubR1*^{H/H} and *BubR1*^{H/H};*p19*^{Arf/-} mice probed with anti-*p16*^{Ink4a} and anti-tubulin antibody. Uncropped images of the scans are shown in Supplementary Information, Fig. S6d. **(g)** Relative expression of *p16*^{Ink4a} in various tissues of 2-month-old *BubR1*^{+/+}, *BubR1*^{H/H} and *BubR1*^{H/H};*p19*^{Arf/-} mice as measured by qRT-PCR. Data are mean \pm s.d. ($n = 3$ males per genotype). All values were normalized to *GAPDH*. Relative expression is to wild-type samples.

BubR1^{H/H};*p16*^{Ink4a/-} mice. Collectively, these data suggest that *BubR1* hypomorphism causes cellular senescence in adipose tissue and skeletal muscle through a *p16*^{Ink4a}-dependent mechanism. As *p16*^{Ink4a} inactivation

attenuates both senescence and ageing in these tissues, the mechanism by which *BubR1* hypomorphism accelerates the ageing phenotypes may involve *p16*^{Ink4a}-induced senescence.

